RSC Chemical Biology

ROYAL SOCIETY OF CHEMISTRY

PAPER

View Article Online
View Journal

Cite this: DOI: 10.1039/d6cb00024j

Methylene insertion reveals the importance of phosphate–phosphate distance in DNase I cleavage

Ayano Nagaya, [a] Kohji Seio [a] and Yoshiaki Masaki *[ab]

Received 27th January 2026,
Accepted 19th April 2026

DOI: 10.1039/d6cb00024j

rsc.li/rsc-chembio

DNase I is a major endonuclease in human serum that cleaves double-stranded DNA. While its activity has been characterized for sequence preference and structural requirements, the effects of chemical modifications on cleavage activity remain underexplored. Here, we report that the insertion of methylene groups at defined positions on DNA substrates significantly changes the DNase I cleavage in a position-dependent manner, leading to either enhancement or suppression depending on the insertion site. These findings indicated that chemical modifications can be used to modulate DNase I activity and suggested that local structure, particularly the distance between phosphate groups, had a significant impact on DNase I cleavage.

Introduction

DNase I is a major endonuclease in human serum that primarily targets double-stranded DNA (dsDNA) and generates 5′-phosphorylated fragments by cleaving the phosphodiester bond between the 3′-hydroxy group and the phosphate.[1–3] Accordingly, avoiding DNase I activity is crucial for the *in vivo* application of DNA-based DDS technologies, such as DNA origami and tetrahedral DNA nanostructures (TDNs),[4–6] HDO (hybrid DNA–RNA oligonucleotides consisting of an ASO and DNA),[7,8] and nucleic-acid-responsive systems including HCR (hybridization chain reaction)[9] and CHA (catalytic hairpin assembly).[10] Chemical modification of oligonucleotides, particularly backbone modifications such as phosphorothioates, has played a central role in improving nuclease resistance and enabling the development of clinically useful nucleic acid therapeutics.[11] Numerous internucleoside linkage modifications have been explored to modulate nuclease susceptibility and influence the biological stability of oligonucleotides.[12] However, strategies to precisely control nuclease activity at defined sites remain limited. Therefore, understanding the cleavage mechanism of DNase I and developing strategies to control its activity are essential for the biological application of DNA-based nucleic acid systems.

Studies on the mechanism of DNase I have shown that the enzyme induces characteristic structural changes in DNA, including bending the duplex by approximately 20° and widening the minor groove by about 3 Å.[13] Consistent with these observations, DNA bendability has been reported to influence DNase I substrate recognition.[14] In addition, differences in minor groove width between B-form and A-form duplexes have been proposed to contribute to differential cleavage activities, and these structural properties are also considered important for understanding the sequence preferences of DNase I.[13]

X-ray crystallographic studies have shown that amino acid residues, such as R111, H134 and H252, recognize the phosphate groups near the cleavage site.[13,15] In addition, the nucleotide located one nucleotide upstream on the 5′ side of the cleavage site plays an important role in sugar moiety recognition by Y76. However, because DNase I forms multiple interactions with DNA, it remains unclear which interactions are most critical for controlling its activity.

We previously reported a method that distinguishes the relative contributions of sugar moiety and phosphate group recognition.[16] This was achieved by comparing the susceptibility to nuclease degradation between methylene groups inserted at either the C5′ or C3′ position (5′-HMT and 3′-HMT, respectively; see Fig. 1). Using this method, we demonstrated that sugar recognition by Q183 and W221 is more important than phosphate recognition in RNase H-mediated cleavage. We assumed that the same approach could be applied to DNase I to evaluate the relative contributions of sugar and phosphate recognition. Therefore, DNA strands containing 5′-HMT and 3′-HMT were synthesized and analyzed using DNase I assays.

[a] *Department of Life Science and Technology, Institute of Science Tokyo, 4259 Nagatsuta, Midori, Yokohama, Kanagawa, 226-8501, Japan. E-mail: ymasaki@life.isct.ac.jp*
[b] *NucleoTIDE and PepTIDE Drug Discovery Center, Institute of Science Tokyo, 1-5-45 Yushima, Bunkyo, Tokyo, 113-8519, Japan*

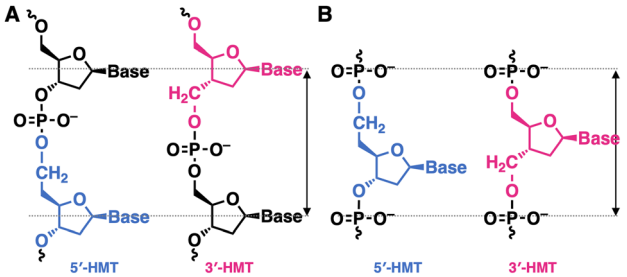

Fig. 1 Extension of the same phosphate distance or the same sugar-moiety distance by 5′-HMT or 3′-HMT. (A) When the 5′-HMT and 3′-HMT positions are shifted by one nucleotide, the same sugar moiety distance is extended.(B) When 5′-HMT and 3′-HMT are installed at the same position, the same phosphate distance is extended.

Materials and methods

General chemistry

All chemical reagents and dry solvents were purchased from Tokyo Chemical Industry, FUJIFILM-Wako Pure Chemical Corporation, Kanto Chemical Co. Inc., Nacalai Tesque, Sigma-Aldrich, and ChemGenes Corporation, and used as received. Phosphoramidite monomers (dA, dC, dG, and dT) were purchased from Glen Research. Recombinant DNase I was purchased from Takara Bio Inc. The Ultrapure™ DNase/RNase-Free Distilled water was purchased from Thermo Fisher Scientific. Reversed-phase HPLC analyses and purifications were performed using a JASCO UV-4070 detector, PU2086 pump, CO4060 column heater and LCNETII/ADC interface system. The columns employed for HPLC were a Waters XBridge C18 column (5 μm, 4.6 × 150 mm) for analytical purposes and a Waters XBridge C18 column (5 μm, 10 × 250 mm) for purification. MALDI-TOF-MS was performed using ultrafleXtreme (Bruker Daltonics). The absorption coefficients of ODNs were calculated according to the nearest-neighbor method using Oligo Analyzer 3.1 (https://sg.idtdna.com/calc/analyzer) by assuming that the molar extinction coefficients of the modified ODNs were identical to those of the unmodified ODN.

Preparation of oligonucleotides

ODNs were synthesized on a 1 μmol scale on solid supports of controlled pore glass (CPG) with a DNA synthesizer nS8-II (Gene Design Inc.) using the standard phosphoramidite method. The DNA phosphoramidites (dA(Bz), dC(Ac), dG(iBu), and dT) and solid supports (Glen Unysupport 1000 and 3′-(6-FAM) CPG) were purchased from Glen Research. Each phosphoramidite was dissolved in anhydrous acetonitrile to obtain a 0.1 M solution. The activator was 0.25 M 5-benzylthio-1*H*-tetrazole (BTT) in acetonitrile (Glen Research). Sulfurization was performed utilizing 0.05 M of ((dimethylamino-methylidene)amino)-3*H*-1,2,4-dithiazaoline-3-thione (DDTT, Chem Genes Corporation) in acetonitrile–pyridine (2 : 3, v/v) for 5 min twice after each coupling step. Unreacted hydroxy groups were capped using tetrahydrofuran/acetic anhydride (Glen Research) and 10% 1-methylimidazole in tetrahydrofuran/pyridine (Glen Research). When the phosphite ester was oxidized to a phosphate group, 1 M *tert*-butyl hydroperoxide in toluene–decane (5 : 1, v/v) was reacted for 2 min. The terminal DMTr group was removed at the final step of synthesis. After synthesis, additional sulfurization was performed for 5 min four times. Each synthesized oligonucleotide was treated with 40% triethylamine in acetonitrile for 30 min at room temperature to remove the cyanoethyl protecting group from the phosphate groups. Cleavage from the CPG solid support was performed using 28% ammonium hydroxide for 1 h at room temperature followed by deprotection of the nucleobases for 18 h at 55 °C. After removal of ammonium hydroxide by a miVac Duo centrifuge evaporator (Genevac, Ipswich, UK), each crude oligonucleotide was purified by reversed-phase HPLC. In this purification, a linear gradient (5–45%, 1% min^{-1}) of solvent I (MeOH) in solvent II (8 mM triethylamine, 100 mM 1,1,1,3,3,3-hexafluoropropan-2-ol buffer) was used at 65 °C at a flow rate of 3.0 mL min^{-1} for 40 min. Purified oligonucleotides were analyzed by reversed-phase HPLC. In this reversed-phase HPLC system, a linear gradient (5–45%, 1% min^{-1}) of solvent I (MeOH) in solvent II (8 mM triethylamine, 100 mM 1,1,1,3,3,3-hexafluoropropan-2-ol buffer) was used at 65 °C at a flow rate of 1.0 mL min^{-1} for 40 min. All the cleavable strands and an uncleavable strand in which the center bases are ''AsA'' (complementary to ON TT) and ''A'' were synthesized as described above, while all the other uncleavable strands were purchased from Fasmac Co., Ltd and used without further purification.

UV melting experiments

UV melting experiments were conducted using a UV-vis spectrophotometer (UV-1900i and TMSPC-8, Shimadzu). Ultrapure™ DNase/RNase-free distilled water was used for all procedures, including dissolution of oligonucleotides and buffer preparation. Each oligonucleotide (400 pmol) was dissolved in 200 μL of folding buffer (10 mM phosphate buffer, pH 7.0, containing 100 mM NaCl and 0.1 mM EDTA). The final duplex concentration was 2.0 μM. The solution was heated at 95 °C for 5 min and slowly cooled to room temperature to allow annealing. The annealed dsDNA solution was placed in the spectrophotometer, and the temperature was increased from 25 °C to 95 °C at 0.5 °C min^{-1}, followed by cooling back to 25 °C at the same rate. Absorbance at 260 nm was recorded to obtain UV melting curves. Measurements were performed in three independent experiments (biological triplicates). The melting curves were smoothed using the Savitzky–Golay method, and melting temperatures (T_m) were determined as the temperature at the maximum of the first derivative of the melting curve. The final T_m value was reported as the average from three independent measurements.

DNase I cleavage assay

3′-FAM-labelled DNA (10 pmol) and the complementary strand (10 pmol) were annealed in 80 μL of annealing buffer containing 50 mM Tris-HCl (pH 7.5) and 0.05 wt% Tween 80. Subsequently, 20 μL of the DNase I solution, containing DNase I (0.1 U or 1 U; recombinant DNase I encoded by the bovine pancreatic DNase I gene and expressed in a non-animal host,

Takara Bio), 50 mM Tris-HCl (pH 7.5), 40 mM $MgCl_2$ and 20 mM DTT, 0.05 wt% Tween 80, was added to the duplex solution (80 μL), and the reaction mixture was incubated at 37 °C for 5 min. The final concentrations were: 100 nM dsDNA, 1 or 10 mU μL^{-1} DNase I, 50 mM Tris-HCl, 8 mM $MgCl_2$, and 4 mM DTT. Aliquots (10 μL each) of the reaction mixture were collected at 2 and 5 min, and quenched by mixing with 10 μL of stop solution containing 10 M urea, 50 mM EDTA·2Na and 0.1 wt% bromophenol blue. The samples were separated on a 20% denaturing polyacrylamide gel at 60 °C for 30 min using a PowerPac HV (Bio-Rad). Gel images were acquired using a Typhoon™ FLA 9500 and analyzed with ImageJ software (v1.54g).

Estimation of the catalytic efficiency ratio (η_{T5}/η_{TT})

The DNase I assay was performed as described above, varying the substrate dsDNA concentration from 0.1 μM to 1 μM. Samples at 0.1 μM were loaded at a standard volume (4 μL). Samples at higher concentrations were diluted prior to loading (two-fold for 0.2 μM, five-fold for 0.5 μM, and ten-fold for 1 μM), and 4 μL of each diluted sample was loaded.

After separating intact and cleaved 3′-FAM-labelled DNA by gel electrophoresis, the band intensities were quantified, and the fraction of cleaved product was calculated as cleaved DNA per (intact DNA + cleaved DNA). The fraction of cleaved product at 2 min was converted to the initial velocity (μM min^{-1}) using the initial substrate concentration ($[S]_0$). The relationship between the initial velocity and substrate concentration was then plotted. For the calculation of the catalytic efficiencies, the initial velocities at 0.1 μM were compared between TT and T5 to determine the ratio η_{T5}/η_{TT}.

Results and discussion

Synthesis

5′-HMT and 3′-HMT phosphoramidites were synthesized through reported procedures.[16–18] Phosphorothioate (PS) linkages are known to be highly resistant to DNase I cleavage because sulfur substitution interferes with metal ion coordination in the active site,[19] whereas adjacent phosphodiester (PO) linkages remain susceptible to hydrolysis.[20] For initial experiments, the oligonucleotides were synthesized with a single PO linkage, while all other internucleotide linkages were PS, thereby restricting the DNase I cleavage site to a single position.

Oligonucleotide names were defined by the two nucleotides immediately adjacent to the PO linkage (Table 1). For example, TT represents an oligonucleotide containing a ToT motif, where o denotes PO linkage. Similarly, AT, GT, CT, TA, TG, and TC denote oligonucleotides containing AoT, GoT, CoT, ToA, ToG, and ToC motifs, respectively. T5 indicates that the second T in the ToT motif is replaced with 5′-HMT. Similarly, A5, G5, and C5 indicate that the second T in the AoT, GoT, and CoT motifs is replaced with 5′-HMT, respectively. Conversely, 3T indicates that the first T in the ToT motif is replaced with 3′-HMT. Likewise, 3A, 3G, and 3C indicate that the first T in the ToA, ToG, and ToC motifs is replaced with 3′-HMT, respectively. Except for the PO motif, all other sequences were identical across the oligonucleotides.

In ooTT, two PS linkages on the 5′-upstream side of the ToT motif in TT are replaced by two additional cleavable PO linkages. Similarly, in ooT5 and oo3T, two PS linkages on the 5′-upstream side are replaced with two PO linkages. Conversely, in TToo, two PS linkages on the 3′-downstream side of the ToT motif in TT are replaced with two PO linkages. Likewise, in T5oo and 3Too, two PS linkages on the 3′-downstream side are replaced with two PO linkages. All oligonucleotides were labelled with a FAM group at the 3′ terminus, allowing cleavage to be detected as the appearance of a lower band on a denaturing polyacrylamide gel.

Before conducting the DNase I assay, we tested to ensure that all the oligonucleotides formed sufficiently stable duplexes. Each oligonucleotide was hybridized with a fully complementary phosphorothioate DNA strand, and the melting temperature (T_m) was measured. The T_m values of the TT, AT, GT and CT duplexes were 52.8 ± 0.10, 53.3 ± 0.26, 55.2 ± 0.10 and 53.9 ± 0.25 °C, respectively. The T_m values of the T5, A5, G5 and C5 duplexes containing 5′-HMT were 49.8 ± 0.06, 51.5 ± 0.25, 54.0 ± 0.20 and 52.1 ± 0.21 °C, respectively. Thus, the effect of the 5′-HMT modifications relative to the corresponding unmodified duplexes (TT, AT, GT and CT) was −3.0, −1.8, −1.2 and −1.8 °C, respectively.

Similarly, the T_m values of the TA, TG and TC duplexes were 52.3 ± 0.26, 55.3 ± 0.25 and 54.1 ± 0.38 °C, respectively. The T_m values of the 3T, 3A, 3G and 3C duplexes containing 3′-HMT were 49.5 ± 0.17, 50.5 ± 0.26, 53.5 ± 0.32 and 52.5 ± 0.40 °C, respectively. Thus, the effect of the 3′-HMT modifications on the corresponding unmodified duplexes (TT, TA, TG and TC) was −3.3, −1.8, −1.8 and −1.6 °C, respectively.

The T_m of the ooTT duplex was 52.8 ± 0.20 °C. The introduction of 5′-HMT or 3′-HMT resulted in T_m values of 51.1 ± 0.06 °C (−1.7 °C) for the ooT5 duplex and 50.9 ± 0.10 °C (−1.9 °C) for the oo3T duplex. Similarly, the T_m of the TToo duplex was 53.0 ± 0.06 °C, whereas the T5oo duplex and 3Too duplex exhibited T_m values of 51.0 ± 0.10 (−2.0 °C) and 50.5 ± 0.31 °C (−2.5 °C), respectively.

Both 5′-HMT and 3′-HMT decreased the duplex stability by approximately 1–2 °C. This observation was consistent with the previous report.[18] Although 5′-HMT and 3′-HMT modifications slightly decreased the T_m values, the observed T_m values were sufficiently high for the DNase I assay.

Experiments using an oligonucleotide which has a single phosphate on the extended site

We conducted a DNase I assay using these oligonucleotides duplexed with fully complementary DNA. All the phosphate groups in the complementary DNA are phosphorothioate linkages, so the complementary strand is expected to be resistant to DNase I cleavage. The reaction was quenched at 1 min intervals by the addition of EDTA, and the samples were analyzed by gel electrophoresis (Fig. 2B). The intensities of the cleavage bands of the unmodified oligonucleotide (TT) and

Table 1 Synthesized oligonucleotide used in this study

Name	Sequence (5′ → 3′)[a]	T_m (°C)	ΔT_m (°C)
TT	CsAsGsTsAsCsAsCsGsCsCsToTsCsTsCsTsAsAsCsCsCsAsF	52.8 ± 0.10	
AT	CsAsGsTsAsCsAsCsGsCsCsAoTsCsTsCsTsAsAsCsCsCsAsF	53.3 ± 0.26	
GT	CsAsGsTsAsCsAsCsGsCsCsGoTsCsTsCsTsAsAsCsCsCsAsF	55.2 ± 0.10	
CT	CsAsGsTsAsCsAsCsGsCsCsCoTsCsTsCsTsAsAsCsCsCsAsF	53.9 ± 0.25	
TA	CsAsGsTsAsCsAsCsGsCsCsToAsCsTsCsTsAsAsCsCsCsAsF	52.3 ± 0.26	
TG	CsAsGsTsAsCsAsCsGsCsCsToGsCsTsCsTsAsAsCsCsCsAsF	55.3 ± 0.25	
TC	CsAsGsTsAsCsAsCsGsCsCsToCsCsTsCsTsAsAsCsCsCsAsF	54.1 ± 0.38	
T5	CsAsGsTsAsCsAsCsGsCsCsToMx0035;sCsTsCsTsAsAsCsCsCsAsF	49.8 ± 0.06	−3.0[b]
A5	CsAsGsTsAsCsAsCsGsCsCsAoMx0035;sCsTsCsTsAsAsCsCsCsAsF	51.5 ± 0.25	−1.8[b]
G5	CsAsGsTsAsCsAsCsGsCsCsGoMx0035;sCsTsCsTsAsAsCsCsCsAsF	54.0 ± 0.20	−1.2[b]
C5	CsAsGsTsAsCsAsCsGsCsCsCoMx0035;sCsTsCsTsAsAsCsCsCsAsF	52.1 ± 0.21	−1.8[b]
3T	CsAsGsTsAsCsAsCsGsCsCs3Mx006F;TsCsTsCsTsAsAsCsCsCsAsF	49.5 ± 0.17	−3.3[c]
3A	CsAsGsTsAsCsAsCsGsCsCs3Mx006F;AsCsTsCsTsAsAsCsCsCsAsF	50.5 ± 0.26	−1.8[c]
3G	CsAsGsTsAsCsAsCsGsCsCs3Mx006F;GsCsTsCsTsAsAsCsCsCsAsF	53.5 ± 0.32	−1.8[c]
3C	CsAsGsTsAsCsAsCsGsCsCs3Mx006F;CsCsTsCsTsAsAsCsCsCsAsF	52.5 ± 0.40	−1.6[c]
ooTT	CsAsGsTsAsCsAsCsGsCoCoToTsCsTsCsTsAsAsCsCsCsAsF	52.8 ± 0.20	
ooT5	CsAsGsTsAsCsAsCsGsCoCoToMx0035;sCsTsCsTsAsAsCsCsCsAsF	51.1 ± 0.06	−1.7[d]
oo3T	CsAsGsTsAsCsAsCsGsCoCo3Mx006F;TsCsTsCsTsAsAsCsCsCsAsF	50.9 ± 0.10	−1.9[d]
TToo	CsAsGsTsAsCsAsCsGsCsCsToToCoTsCsTsAsAsCsCsCsAsF	53.0 ± 0.06	
T5oo	CsAsGsTsAsCsAsCsGsCsCsToMx0035;oCoTsCsTsAsAsCsCsCsAsF	51.0 ± 0.10	−2.0[e]
3Too	CsAsGsTsAsCsAsCsGsCsCs3Mx006F;ToCoTsCsTsAsAsCsCsCsAsF	50.5 ± 0.31	−2.5[e]
5T	CsAsGsTsAsCsAsCsGsCsCsMx0035;oTsCsTsCsTsAsAsCsCsCsAsF	—	—

[a] Uppercase letters indicate DNA, "s" indicates phosphorothioate linkages, "o" indicates phosphate linkage, "5" indicates 5′-HMT, "3" indicates 3′-HMT. Underlined "Mx006F;" or "Mx0073;" is the extended phosphate or phosphorothioate site. All oligonucleotides in this list are modified with FAM at the 3′-end, indicated by "F". (b)–(e) ΔT_m values relative to the corresponding unmodified control oligonucleotides. [b] For T5, A5, G5, and C5, the corresponding controls are TT, AT, GT, and CT, respectively. [c] For 3T, 3A, 3G, and 3C, the corresponding controls are TT, TA, TG, and TC, respectively. [d] For ooT5 and oo3T, the corresponding control is ooTT. [e] For T5oo and 3Too, the corresponding control is TToo.

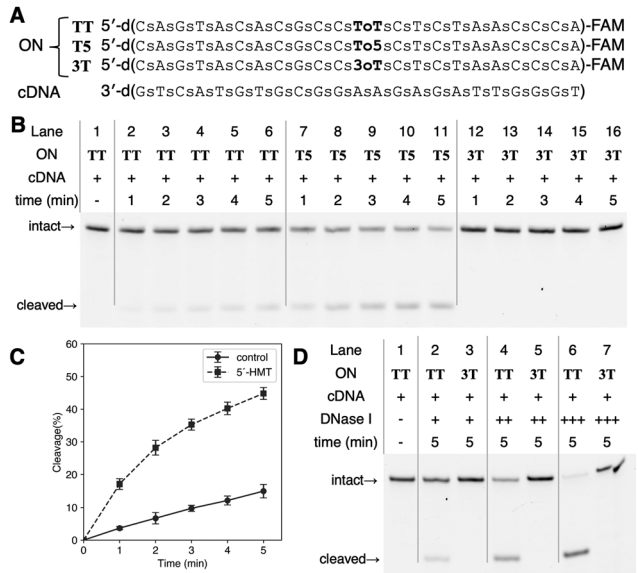

Fig. 2 (A) Sequences of oligonucleotides used in this study. (B) Cleavage of oligonucleotides containing 5′-HMT or 3′-HMT. Reactions were performed in 50 mM Tris–HCl (pH 7.5) containing 8 mM $MgCl_2$, 5 mM DTT, 0.05% Tween 80, and 100 nM DNA, with DNase I at 1 mU μL^{-1}. (C) Time-dependent cleavage of unmodified DNA (solid line with circle markers) and DNA containing 5′-HMT (dashed line with square markers). (D) Inhibitory effect of 3′-HMT on DNase I activity. DNase I +: 1 mU μL^{-1}, ++: 10 mU μL^{-1}, and +++: 100 mU μL^{-1}.

the 5′-HMT-containing strand (T5) increased over time. After 5 min, the cleavage of T5 reached 45%, whereas that of TT was 15% (Fig. 2C).

We varied the substrate concentration ($[S]_0$) and examined its relationship with the initial velocity (v_0) (Fig. S3). Both TT and T5 showed the linear dependence of v_0 on $[S]_0$ in the range of 0.1–1 μM, supporting analysis under conditions where $[S]_0 \ll K_m$. The ratio of the catalytic efficiencies η (k_{cat}/K_m) of TT and T5 was determined from the initial rates measured at 0.1 μM. The resulting ratio (η_{T5}/η_{TT}) was 4.2, indicating an approximately four-fold increase in catalytic efficiency.

In contrast, the 3′-HMT-containing strand (3T) showed no detectable cleavage by DNase I. Even when the amount of DNase I was increased ten-fold (Fig. 2D, lane 5) or one hundred-fold (Fig. 2D, lane 7), no cleavage products were observed.

Sequence preference

To examine whether the same effect is observed in other sequences, we changed the nucleotides adjacent to the modification and annealed each oligonucleotide with its fully complementary strand to form a duplex. At a reaction time of 5 min, the cleavage percentages of the control TT, AT, GT, and CT duplexes were 10%, 7%, 3%, and 4%, respectively (Fig. 3A, lanes 3, 7, 11, and 15). The cleavage percentages of the T5, A5, G5, and C5 duplexes were 41%, 44%, 25%, and 26%, respectively. All duplexes containing 5′-HMT were cleaved more rapidly than their corresponding unmodified oligonucleotides (Fig. 3A, lanes 5, 9, 13, and 17).

We also examined the cleavage activity of oligonucleotides in which the 3′-downstream nucleotide adjacent to the 3′-HMT modification was changed to A, G, or C. To enhance the cleavage reaction, DNase I concentration was increased from 1 mU to 10 mU μL^{-1}. Under this condition, the cleavage

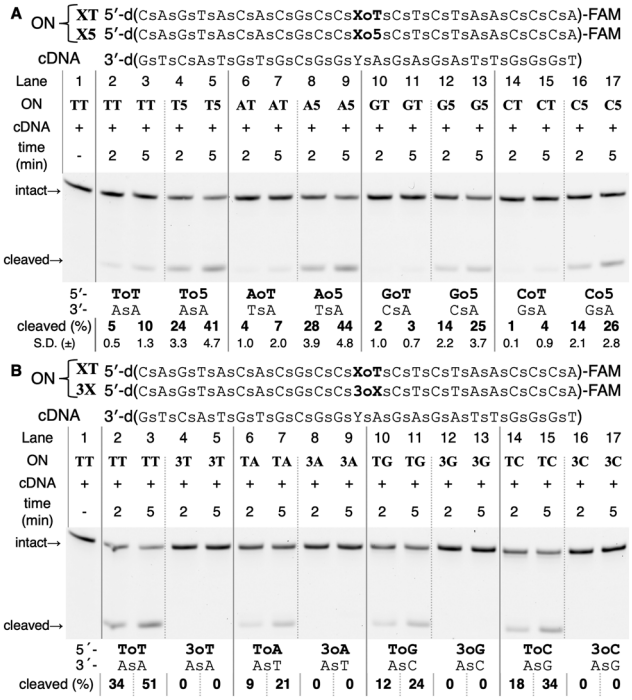

Fig. 3 DNase I assays using various base pairs. Reactions were carried out in 50 mM Tris–HCl (pH 7.5) with 8 mM $MgCl_2$, 5 mM DTT, 0.05% Tween 80, and 100 nM DNA. The DNase I concentrations were 1 mU μL^{-1} for (A) and 10 mU μL^{-1} for (B) (lanes 2–17). S.D. = standard deviation.

percentages of the control TT, AT, GT, and CT duplexes at 5 min were 51%, 21%, 24%, and 34%, respectively (Fig. 3B, lanes 3, 7, 11, and 15). While cleavage was observed for all unmodified duplexes (TT, TA, TG, and TC), duplexes containing 3′-HMT (3T, 3A, 3G, and 3C) showed no detectable DNase I cleavage under these conditions (Fig. 3B, lanes 5, 9, 13, and 17).

Experiments with oligonucleotides bearing additional phosphates around the extended site

To investigate how 5′-HMT and 3′-HMT influence the local interactions around the DNase I active site, we performed cleavage assays using the oligonucleotides ooTT, TToo, ooT5, T5oo, oo3T and 3Too. Each oligonucleotide was hybridized with a complementary DNA strand prior to the assay. The phosphate corresponding to the methylene-inserted phosphate linkage was designated as position 0, with the 5′ upstream phosphates defined as −1 and −2, and the 3′ downstream phosphates as +1 and +2.

In assays using unmodified oligonucleotides, ooTT was cleaved at positions −1 and 0 (Fig. 4A, lanes 2 and 3), whereas TToo was cleaved at positions 0 and +1 (Fig. 4A, lanes 4 and 5). It should be noted that DNase I exhibits neither 5′-to-3′ nor 3′-to-5′ exonuclease activity.[21] Therefore, cleavage at positions −1 and 0, as well as at positions 0 and +1, could be considered independent endonucleolytic events.

The 5′-HMT-modified oligonucleotides were evaluated under the same conditions (Fig. 4A, lanes 6–9). ooT5 duplex was cleaved exclusively at position 0, whereas T5oo was cleaved

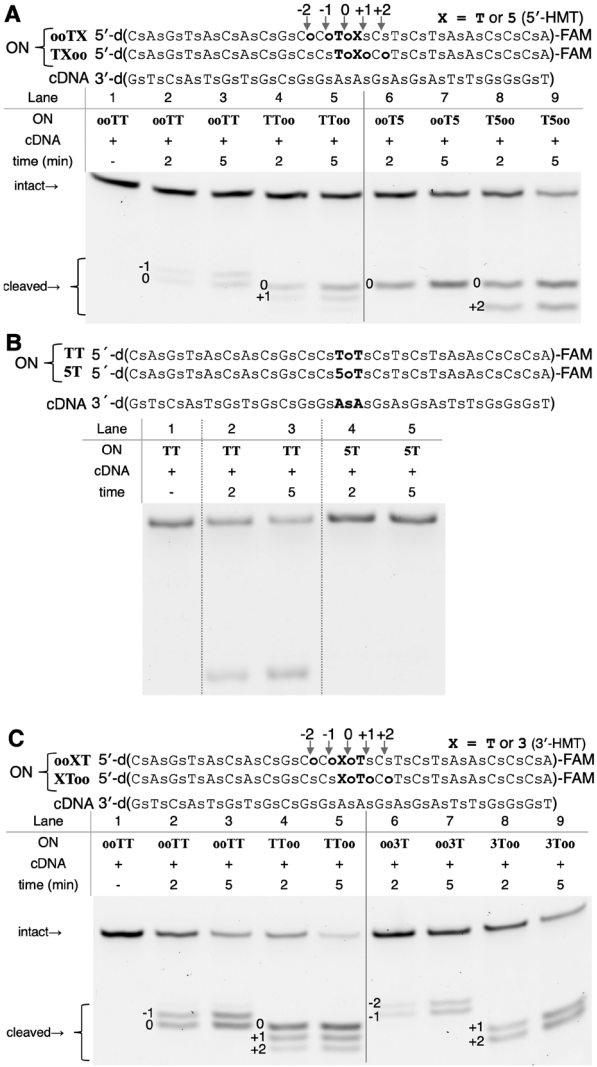

Fig. 4 (A) Effect of 5′-HMT on DNase I cleavage at adjacent phosphates. (B) Effect of 5′-HMT on the phosphate located downstream of the extended site. (C) Effect of 3′-HMT on DNase I cleavage at adjacent phosphates. All reactions were carried out in Tris-HCl (pH7.5) 50 mM, $MgCl_2$ 8 mM, DTT 5 mM, Tween 80 0.05% and DNA 100 nM. DNase I concentrations were 1 mU μL^{-1} for (A) and 10 mU μL^{-1} for (B) and (C).

at positions 0 and +2. Notably, no cleavage at position +1 was detected. To confirm whether cleavage at the +1 position is indeed suppressed, we synthesized the 5T oligonucleotide, in which DNase I cleavage occurs only at the +1 position. The susceptibility of the 5T duplex to DNase I cleavage was then examined. As a result, no cleavage was observed for the 5T duplex (Fig. 4B).

In the case of duplexes containing 3′-HMT, the cleavage reactions were slower. Therefore, assays were performed using a ten-fold higher concentration of DNase I. The results for the unmodified controls under this condition are shown in Fig. 4C, lanes 2–5. The ooTT duplex was cleaved at positions 0 and −1, whereas the TToo duplex was cleaved at positions 0, +1 and +2. Even under these conditions, the oo3T duplex showed complete suppression of cleavage at position 0, with only minor cleavage

at positions −1 and −2 (Fig. 4C, lanes 6 and 7). Similarly, the 3Too duplex exhibited full inhibition of cleavage at position 0, while cleavage at positions +1 and +2 was observed (Fig. 4C, lanes 8 and 9).

At 5 min, the ooTT duplex retained 32% intact substrate, whereas the oo3T duplex retained 75%. Similarly, the TToo duplex and 3Too duplex showed 15% and 38% intact substrate, respectively (Fig. 4C, lanes 3, 5, 7, and 9). Taken together, these results suggested that even a single 3′-HMT modification can reduce DNase I-mediated cleavage, even when the surrounding phosphates are unmodified.

We assumed that inhibiting the interaction most critical for DNase I cleavage would lead to the strongest suppression of activity. Insertion of a methylene group into the phosphate backbone using 5′-HMT or 3′-HMT increases both the phosphate–phosphate distance and the sugar–sugar distance in different ways. Therefore, by comparing the effects of these modifications, we could gain insight into the key interactions involved in DNase I cleavage. The interaction sites between the cleavage products and DNase I are illustrated in Fig. 5.

The positions of H252 and H134, which interact directly at the cleavage site, were fixed, and the surrounding interaction residues R111 and Y76 were included based on previous reports.[13] In the case of 5′-HMT, methylene insertion is expected to shift the relative positions of the interactions with R111 and Y76 for the +1 cleavage product. In contrast, for 3′-HMT, methylene insertion is expected to abolish interactions with R111 and Y76 for the 0-cleavage product, whereas interaction with Y76 is expected to be lost for the +1-cleavage product.

Our results showed that neither the +1-cleavage product for 5′-HMT nor the 0-cleavage product for 3′-HMT was observed, whereas the +1-cleavage product for 3′-HMT was detected. These observations suggested that the phosphate–phosphate distance associated with the interaction between the cleavage site and R111 is particularly important for DNase I activity.

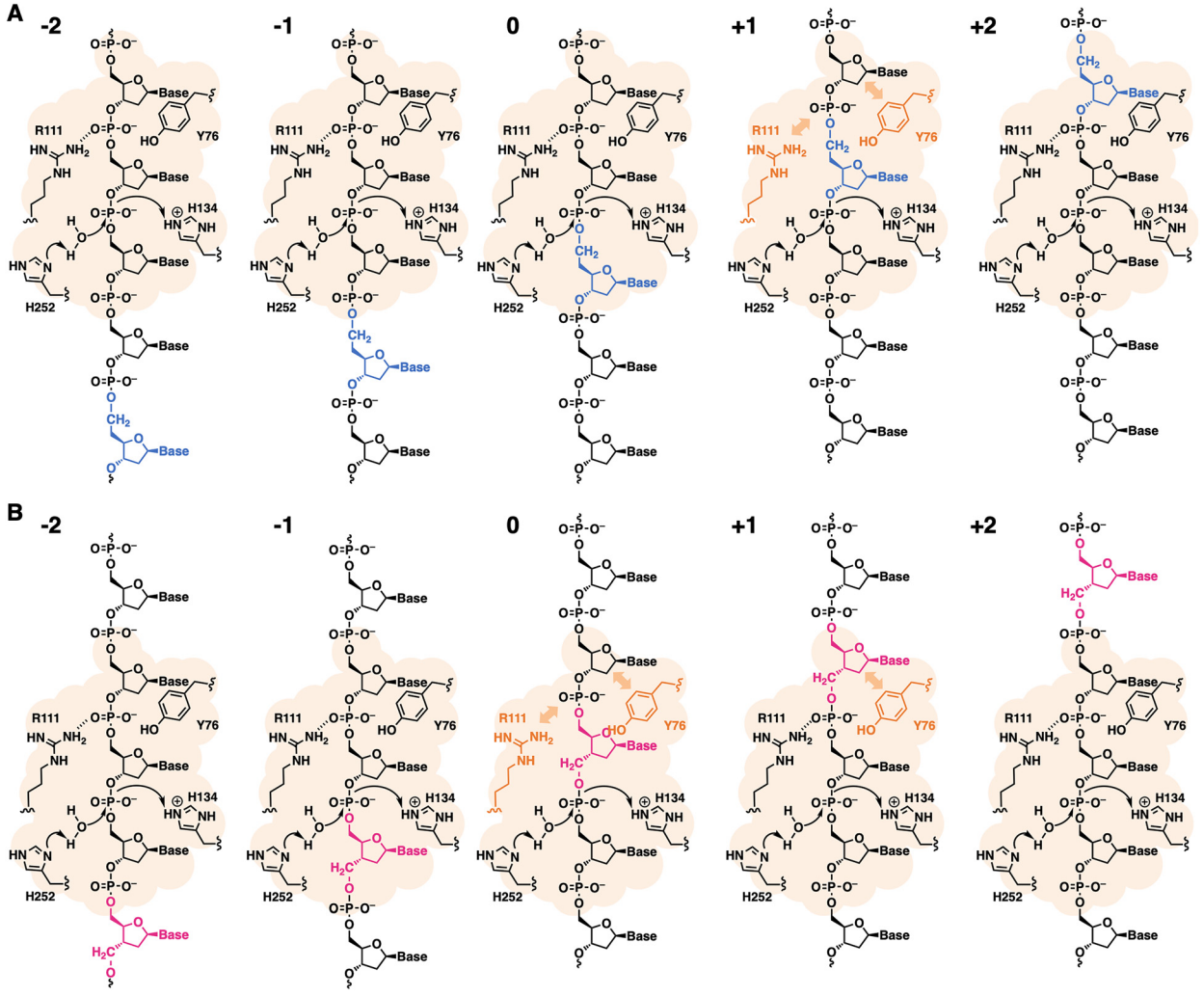

Fig. 5 Positions of the modified nucleoside relative to the cleavage site for each cleavage product. (A) Cleavage of oligonucleotides containing 5′-HMT. (B) Cleavage of oligonucleotides containing 3′-HMT. Blue and red indicate 5′-HMT and 3′-HMT, respectively. Amino acid residues shown in orange indicate residues whose native interactions with DNA are expected to be disrupted when amino acid interactions at the cleavage site are fixed. Regions highlighted in orange are close to DNase I.

DNase I is known to require Ca^{2+} and Mg^{2+} ions for its cleavage activity. Although the precise positions of metal ion coordination have not been experimentally determined, it has been proposed that the metal ions coordinate with the non-bridging oxygen atoms of the scissile PO linkage.[22,23] Because cleavage occurs only at PO linkages in this study, metal ion coordination at the cleavage site is expected to be similar across all substrates.

Our study has a limitation. In our experimental design, elongation of the phosphate–phosphate distance occurs at the same phosphate pair for both 5′-HMT and 3′-HMT modifications. At the same time, methylene insertion may also increase local flexibility of the sugar moiety due to the loss of the *gauche* effect. However, DNase I cleavage is generally known to preferentially occur at more bendable regions of DNA.[24] If increased sugar flexibility were a dominant factor, an enhancement rather than inhibition of cleavage would be expected. In contrast, cleavage was strongly suppressed in our experiments. These observations suggested that sugar flexibility upstream of the cleavage site is unlikely to be a major determinant of DNase I cleavage.

Although methylene insertion has primarily been employed to enhance enzymatic resistance,[18,25] we observed accelerated DNase I cleavage upon 5′-HMT insertion downstream of the phosphate at the cleavage site, independent of sequence context. We speculated that this behavior may reflect changes in local nucleic acid bending properties induced by methylene insertion. DNase I has been widely used as a probe for DNA bendability.[24] Thus, enhanced local flexibility or pre-bending could facilitate productive enzyme–substrate interactions at specific positions. To further examine the relationship between DNA flexibility and DNase I cleavage, a methylene group was introduced into a bulged region to increase local bendability (Fig. S4). However, no further acceleration of cleavage was observed. Instead, cleavage was suppressed under these duplexes. These results suggest that excessive structural distortion is not favorable for DNase I activity. Taken together, these observations suggested that DNase I activity is influenced by local, position-dependent structural features, and that excessive structural distortion is unfavorable for cleavage.

Conclusions

In this study, we systematically evaluated the effects of position-specific methylene insertion into phosphate linkages on DNase I activity. Analysis of positions at which cleavage was completely suppressed suggested the importance of the phosphate–phosphate distance upstream of the cleavage site and highlighted a critical role of the interaction with R111 in DNase I recognition.

Although methylene insertion has generally been employed to enhance resistance to enzymatic degradation, to the best of our knowledge, this study is the first to demonstrate that methylene insertion can also promote DNase I-mediated cleavage depending on its position. These findings provide a useful framework for the development of nucleic acid-based technologies through precise control of DNA structure and enzymatic activity.

Author contributions

Conceptualization, A.N., K.S. and Y.M.; methodology, A.N. and Y.M.; investigation, A.N. and Y.M.; writing – original draft, A.N.; writing – review and editing, A.N., K.S. and Y.M.; funding acquisition, K.S. and Y.M.; resources, K.S. and Y.M.

Conflicts of interest

There are no conflicts to declare.

Data availability

The data supporting this paper have been included as part of the supplementary information (SI). Supplementary information is available. See DOI: https://doi.org/10.1039/d6cb00024j.

Acknowledgements

This work was supported by the JST FOREST program (Grant No. JPMJFR2223), Japan. This work was also partially supported by the Japan Agency for Medical Research and development (Grant No. 24fk0210147h0001 and 25fk0210181h0001). We thank the Materials Analysis Division, Open Facility Center, Institute of Science Tokyo, for their support with the MALDI-TOF-MS. We thank the Open Research Facilities for Life Science and Technology at the Institute of Science Tokyo for their technical assistance.

Notes and references

1 D. Nadano, T. Yasuda and K. Kishi, *Clin. Chem.*, 1993, **39**, 448–452.
2 J. D. Love and R. R. Hewitt, *J. Biol. Chem.*, 1979, **254**, 12588–12594.
3 J. D. Smith and R. Markham, *Nature*, 1952, **170**, 120–121.
4 P. W. K. Rothemund, *Nature*, 2006, **440**, 297–302.
5 R. P. Goodman, R. M. Berry and A. J. Turberfield, *Chem. Commun.*, 2004, 1372–1373.
6 R. Duangrat, A. Udomprasert and T. Kangsamaksin, *Cancer Sci.*, 2020, **111**, 3164–3173.
7 K. Nishina, W. Piao, K. Yoshida-Tanaka, Y. Sujino, T. Nishina, T. Yamamoto, K. Nitta, K. Yoshioka, H. Kuwahara, H. Yasuhara, T. Baba, F. Ono, K. Miyata, K. Miyake, P. P. Seth, A. Low, M. Yoshida, C. F. Bennett, K. Kataoka, H. Mizusawa, S. Obika and T. Yokota, *Nat. Commun.*, 2015, **6**, 7969.
8 Y. Asami, T. Nagata, K. Yoshioka, T. Kunieda, K. Yoshida-Tanaka, C. F. Bennett, P. P. Seth and T. Yokota, *Mol. Ther.*, 2021, **29**, 838–847.

9 K. Morihiro, H. Osumi, S. Morita, T. Hattori, M. Baba, N. Harada, R. Ohashi and A. Okamoto, *J. Am. Chem. Soc.*, 2023, **145**, 135–142.
10 S. Yue, X. Song, W. Song and S. Bi, *Chem. Sci.*, 2019, **10**, 1651–1658.
11 A. Khvorova and J. K. Watts, *Nat. Biotechnol.*, 2017, **35**, 238–248.
12 G. Clavé, M. Reverte, J.-J. Vasseur and M. Smietana, *RSC Chem. Biol.*, 2021, **2**, 94–150.
13 A. Lahm and D. Suck, *J. Mol. Biol.*, 1991, **222**, 645–667.
14 M. E. Hogan, M. W. Roberson and R. H. Austin, *Proc. Natl. Acad. Sci. U. S. A.*, 1989, **86**, 9273–9277.
15 S. A. Weston, A. Lahm and D. Suck, *J. Mol. Biol.*, 1992, **226**, 1237–1256.
16 Y. Masaki, A. Tabira, S. Hattori, S. Wakatsuki and K. Seio, *Org. Biomol. Chem.*, 2022, **20**, 8917–8924.
17 Y. S. Sanghvi, R. Bharadwaj, F. Debart and A. De Mesmaeker, *Synthesis*, 1994, 1163–1166.
18 T. Kofoed, P. B. Rasmussen, P. Valentin-Hansen and E. B. Pedersen, *Acta Chem. Scand.*, 1997, **51**, 318–324.
19 F. Eckstein, *Nucleic Acid Ther.*, 2014, **24**, 374–387.
20 S. Spitzer and F. Eckstein, *Nucleic Acids Res.*, 1988, **16**, 11691–11704.
21 S. Cal, K. L. Tan, A. McGregor and B. A. Connolly, *EMBO J.*, 1998, **17**, 7128–7138.
22 S. J. Jones, A. F. Worrall and B. A. Connolly, *J. Mol. Biol.*, 1996, **264**, 1154–1163.
23 M. Guéroult, D. Picot, J. Abi-Ghanem, B. Hartmann and M. Baaden, *PLoS Comput. Biol.*, 2010, **6**, e1001000.
24 I. Brukner, R. Sánchez, D. Suck and S. Pongor, *EMBO J.*, 1995, **14**, 1812–1818.
25 K. Yamada, V. N. Hariharan, J. Caiazzi, R. Miller, C. M. Ferguson, E. Sapp, H. H. Fakih, Q. Tang, N. Yamada, R. C. Furgal, J. D. Paquette, A. Biscans, B. M. Bramato, N. McHugh, A. Summers, C. Lochmann, B. M. D. C. Godinho, S. Hildebrand, S. O. Jackson, D. Echeverria, M. R. Hassler, J. F. Alterman, M. DiFiglia, N. Aronin and A. Khvorova, *Nat. Biotechnol.*, 2025, **43**, 904–913.